

# Thermogravimetry of manganese dioxides<sup>1</sup>

Rudolf Giovanoli

*Laboratory of Electron Microscopy, Institute of Inorganic Chemistry of the University of Berne, P.O.B. 906, CH-3000 Berne 9 (Switzerland)*

(Received 8 December 1992; accepted 21 January 1993)

## Abstract

A number of manganese dioxides have been synthesized and investigated by X-ray diffraction, electron microscopy and thermogravimetry under flowing oxygen.

The TG curves show, (a) water loss, (b) release of OH-water, and (c) oxygen release. The water loss is negligible for fully crystalline  $\beta$ -MnO<sub>2</sub> and the significant main step is due to the transformation to  $\alpha$ -Mn<sub>2</sub>O<sub>3</sub>. However,  $\gamma$ - and  $\epsilon$ -MnO<sub>2</sub> exhibit a remarkable mass loss long before the main step occurs. Phyllo-manganates also show high water loss and the nucleation of new phases.

Comparison of the various water loss curves reveals that three types of water are present. (i) Adsorbed (loosely bound) molecular water which desorbs from 25 to 105°C. (ii) Interlayer water which in phyllo-manganates is still molecular but more tightly bound. It is released at temperatures overlapping with those of adsorption water release but extending up to 150–250°C. (iii) The condensation of OH-groups in  $\gamma$ - and  $\epsilon$ -MnO<sub>2</sub> leads to the release of much more tightly bound water (which we call OH-water) from 105 to 500°C and even higher. The release of OH-water is accompanied by the nucleation of  $\beta$ -MnO<sub>2</sub>.

Battery active material has some adsorbed molecular water but the significant feature is the presence of OH groups and an equivalent amount of Mn<sup>3+</sup> ions in the lattice. Vacancies are a characteristic feature.

Thermogravimetry in combination with X-ray diffraction and electron microscopy is shown to be a valuable means of characterising MnO<sub>2</sub>.

## 1. INTRODUCTION

Manganese dioxides (German common name “Braunstein”) were thoroughly investigated for the first time by Glemser and co-workers [1–3]. Some TG results were included. We took up the subject ten years later and reported preparation, characterization and reactions of these compounds [4–9]. In parts of the investigation we also used thermogravimetry but were limited by available equipment. Fifteen years further on we have again

<sup>1</sup> Dedicated to Hans Georg Wiedemann.

begun to investigate the thermogravimetric behaviour of  $\text{MnO}_2$  on which we report here.

## 2. EXPERIMENTAL

### 2.1. Preparation of samples

#### 2.1.1. Fully crystalline $\beta\text{-MnO}_2$

Pure and fully crystalline  $\beta\text{-MnO}_2$  in globular particles of 50–150  $\mu\text{m}$  diameter was obtained from Baker (No. 0170). The actual crystallites are smaller. The X-ray powder diffraction lines show no broadening; therefore the crystallite size is larger than 2000  $\text{\AA}$  (Fig. 1(a)).

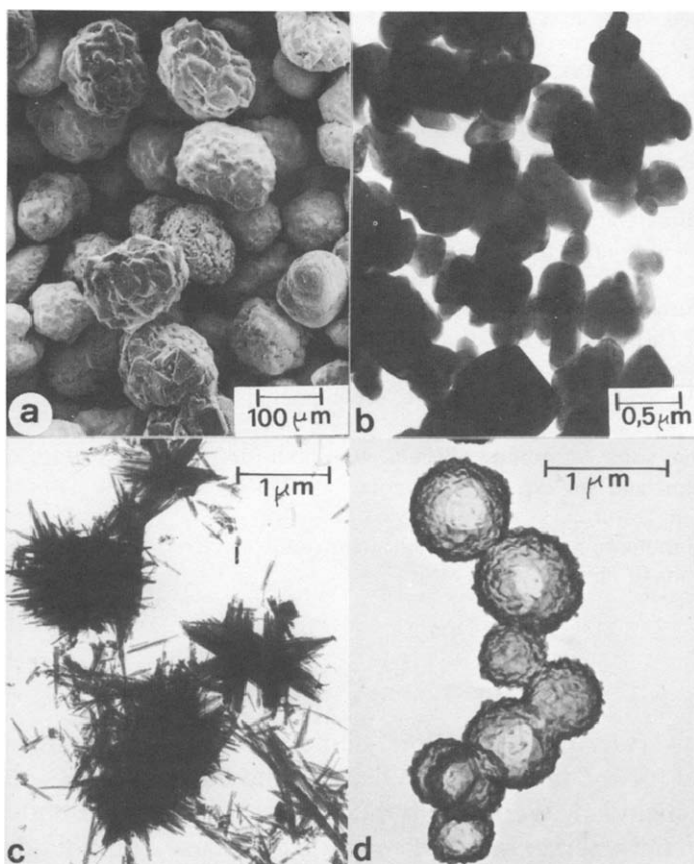


Fig. 1. Electron micrographs of four of the investigated products: (a) Scanning electron micrograph of  $\beta\text{-MnO}_2$  (Baker 0170). (b) Transmission electron micrograph of refluxed  $\beta\text{-MnO}_2$ . (c) Transmission electron micrograph of  $\gamma\text{-MnO}_2$  (Faradizer WS). (d) Transmission electron micrograph of a carbon replica of  $\epsilon\text{-MnO}_2$  (ozone method). Ageing of this product leads to outgrowths of the globular aggregates and formation of needles of  $\gamma\text{-MnO}_2$ .

### 2.1.2. $\beta$ - $MnO_2$ by refluxing

A  $\beta$ - $MnO_2$  variety with smaller crystallites can be prepared by refluxing  $Mn_3O_4$  or  $\gamma$ - $MnO_2$  in 2 N  $HNO_3$  for 2–6 months at 98°C. The crystallite size is about 2000 Å (Fig. 1(b)).

### 2.1.3. $\gamma$ - $MnO_2$ (commercial)

$\gamma$ - $MnO_2$  is a commercial product of Sedema (Tertre, Belgium) of trade name Faradiser WS. It consists of agglomerations of needles about 0.5–1  $\mu$ m long and about 400 Å broad and thick (Fig. 1(c)).

### 2.1.4. $\gamma$ - $MnO_2$ from 7 Å phyllomanganate

$\gamma$ - $MnO_2$  was prepared by tempering  $Na_4Mn_{14}O_{27} \cdot 9H_2O$  in the furnace for 22 h at 350°C and subsequent refluxing in 2 N  $HNO_3$  for 3 days at 98°C. The product consisted of prisms of about 1  $\mu$ m length and approximately 1000 Å broad and 500 Å thick.

### 2.1.5. $\epsilon$ - $MnO_2$ (commercial and ozone method)

$\epsilon$ - $MnO_2$  is commercially available from Sedema (Tertre, Belgium) under the trade name Faradiser M. We prepared it by precipitation from a 0.7 M solution of  $Mn(NO_3)_2 \cdot 4H_2O$  in 3 M  $HNO_3$  by bubbling through an air flow of about 150 ml  $min^{-1}$  containing 2.2%  $O_3$ . The substance consists of spherulites of 1–2  $\mu$ m diameter consisting of platelets 1000 Å across and 200 Å thick (Fig. 1(d)).

### 2.1.6. Na-7 Å phyllomanganate $Na_4Mn_{14}O_{27} \cdot 9H_2O$

$Na_4Mn_{14}O_{27} \cdot 9H_2O$  was prepared by fast oxygenation of freshly precipitated  $Mn(OH)_2$  in suspension at high pH as described in ref. 6. The product consists of platelets about 1  $\mu$ m across and about 200–400 Å thick.

### 2.1.7. K-7 Å phyllomanganate (“ $\delta$ - $MnO_2$ ” after Glemser et al. [1])

$\delta$ - $MnO_2$  was prepared by adding 100 ml of a 2% solution of  $KMnO_4$  to a boiling solution of 50 g KBr and 10 ml conc. HAc in 1 l  $H_2O$ . Glemser et al. [1] originally used NaBrO but we found that NaBr and KBr may be used instead. The product shows spherulites of approximate diameter 2500 Å consisting of platelets about 1000 Å in diameter and about 100 Å thick.

### 2.1.8. Z-disordered ( $z_0$ ) phyllomanganate (after Murray [10])

Z-disordered phyllomanganate was prepared by adding a solution of 5.9 g  $MnCl_2$  in 500 ml  $H_2O$  dropwise to a solution of 0.9 g  $NaMnO_4$  or  $KMnO_4$  and 0.5 g NaOH in 31  $H_2O$ . The product is nearly amorphous in X-ray diffraction and shows only two very broad reflections near 2.44 and 1.44 Å. It consists of 1–3  $\mu$ m diameter aggregates of ultrathin platelets (about 50 Å thick) of approximate diameter 100–200 Å.

## 2.2. X-Ray diffraction

Samples were studied by X-ray diffraction using a Guinier–De Wolff camera of a Nonius–Enraf Mark IV apparatus with Fe  $K\alpha_1$  radiation and 6 h exposure time.

## 2.3. Electron microscopy

Samples were dispersed in twice distilled  $H_2O$  and a drop of the suspension was dried on a carbon coated bronze grid. A Hitachi H-600-2 transmission electron microscope with EDX attachment Tracor TN 5402 was used. For low magnifications we used a Jeol JSM-840 scanning electron microscope with the same EDX attachment. Samples for the scanning mode were glued on a specimen holder and sputtered with about 400 Å gold. A “Standardless Quantitative” analysis program was used for elemental analysis in the scanning microscope.

## 2.4. Thermogravimetry

We used a Mettler TA 4000 system with processor TC 11, furnace TG 50 and microbalance M 3. Results were evaluated using Mettler Graphware 72.5. The atmosphere was usually flowing  $O_2$  (about  $50\text{ ml min}^{-1}$ ) and in some instances air in  $N_2$ . Sample size was about 20–35 mg, placed in corundum crucibles of  $70\ \mu\text{l}$  volume.

# 3. RESULTS

## 3.1. Thermogravimetry

### 3.1.1. $\beta\text{-MnO}_2$ (Baker no. 0170)

This fully crystalline  $MnO_2$  had to be crushed in an agate mortar for TG. It released less than 0.1% adsorbed water from 25–100°C and the main step (9.20%) with DTG minimum at 609°C occurred between 400 and 700°C leading to  $\alpha\text{-Mn}_2\text{O}_3$  for which the calculated mass loss would be 9.202%. In flowing oxygen this phase was stable up to 900–950°C where the transition to  $Mn_3O_4$  is just about to begin. From 105–400°C a slight mass loss (0.1%) was also observed.

### 3.1.2. $\beta\text{-MnO}_2$ (refluxed)

The shape of this TG curve was nearly identical to that of the Baker  $\beta\text{-MnO}_2$  but the release of adsorbed water was higher (0.29%). Also there was greater mass loss from 105–400°C (0.27%). The main step was a loss of 9.42%.

### 3.1.3. $\gamma$ - $MnO_2$ (Faradiser WS)

The mass loss from 25–105°C was again higher (0.98%) as was the loss from 105–500°C (2.40%). The main step occurred earlier than with  $\beta$ - $MnO_2$ , i.e. with DTG minimum at 565°C and 7.97% mass loss. At the end of the runs no sign of incipient  $Mn_2O_4$  nucleation was observed.

### 3.1.4. $\gamma$ - $MnO_2$ (refluxed)

The mass loss from 25–105°C was considerably higher than in  $\beta$ - $MnO_2$  (0.78%). Also the mass loss from 105–400°C was much higher (2.22%) and the main step occurred earlier (DTG minimum at 561°C). Just at the end of the run  $Mn_3O_4$  begins to form. These results are close to those of Faradiser WS.

### 3.1.5. $\varepsilon$ - $MnO_2$ (Faradiser M)

The loss of mass from 25–105°C was 1.64%, i.e. higher than in  $\gamma$ - and  $\beta$ - $MnO_2$ . The main step with DTG minimum at 557°C occurred in a range comparable with that of  $\gamma$ - $MnO_2$  but it was only 7.46%. At the end of the run no  $Mn_3O_4$  was observed.

### 3.1.6. $\varepsilon$ - $MnO_2$ (ozone method)

The mass loss from 25–105°C was much higher than in  $\gamma$ - or  $\beta$ - $MnO_2$  (4.51%). It was also higher compared to Faradiser M which was obviously better dried. The loss from 105 to 500°C was 6.31% and the main step took place at lower temperature than in Faradiser M (DTG minimum at 557°C) and was smaller (6.31%). At the end of the run at 1000°C the nucleation of  $Mn_2O_4$  begins.

### 3.1.7. $Na$ -7 Å phyllomanganate $Na_4Mn_{14}O_{27} \cdot 9H_2O$

This phase lead to TG measurements totally different from those described above. The main loss of mass took place at the beginning and extended to 150°C. A much smaller step was observed around 450–550°C and only after 840°C did another important reaction take place.

### 3.1.8. 7 Å Phyllomanganate (Glemser et al. [1])

This finely divided phase followed the pattern described in Section 3.1.7 with a big step right from the beginning up to 300°C and a smaller step from 300 to 450°C. A slight mass increase followed from 450 to 500°C. Three more steps were observed after 700°C.

### 3.1.9. $Z_d$ Phyllomanganate

This finely divided near-amorphous phase behaved similarly to Glemser's product with a pronounced step at the beginning up to 300°C. A

TABLE 1  
TG results for  $\beta$ -,  $\gamma$ - and  $\epsilon$ -MnO<sub>2</sub>

Substance	Ads. H <sub>2</sub> O (25–105°C)/%	OH <sup>-</sup> -water/%	Main step/%	DTG min./°C
$\beta$ -MnO <sub>2</sub> (Baker)	0.07	0.06	9.22	609
$\beta$ -MnO <sub>2</sub> (refluxed)	0.15	0.27	9.42	609
$\gamma$ -MnO <sub>2</sub> (Faradiser WS)	0.98	2.40	7.97	565
$\gamma$ -MnO <sub>2</sub> (refluxed)	0.78	2.22	8.43	561
$\epsilon$ -MnO <sub>2</sub> (Faradiser M)	1.64	2.93	7.46	557
$\epsilon$ -MnO <sub>2</sub> (O <sub>3</sub> method)	4.51	6.31	6.91	537

TABLE 2  
TG results for phyllo-manganates

Substance	Adsorbed and interlayer H <sub>2</sub> O/%	Main step/%	DTG min./°C
Na <sub>4</sub> Mn <sub>14</sub> O <sub>27</sub> · 9H <sub>2</sub> O 7 Å phyllo-manganate	11.85	2.08	905
(Glemser's "δ")	14.27	2.62	769
z <sub>4</sub> manganate (Murray)	22.09	3.36	785

much smaller mass loss was observed at 300–500°C and two more steps followed after 650°C.

These results are summarized in Tables 1 and 2 and Fig. 2.

### 3.2. X-Ray diffraction

The most important mineral species observed was  $\alpha$ -Mn<sub>2</sub>O<sub>3</sub>. It usually appeared after the main step around 500–600°C. Mn<sub>3</sub>O<sub>4</sub> turned up near 1000°C in a few cases (see above) and it was regularly the only product in flowing N<sub>2</sub>. This simple scheme was followed by  $\beta$ -MnO<sub>2</sub>.

More complicated events show up with  $\gamma$ - and  $\epsilon$ -MnO<sub>2</sub>. We have reported earlier [11] that isothermal treatment ("roasting" as an industrial process) can lead to nucleation of undesired  $\beta$ -MnO<sub>2</sub> after 4 h at 300°C. Under dynamic conditions this is also the case with a heating rate of 5°C min<sup>-1</sup> in O<sub>2</sub> up to 500°C. The 110 reflection of  $\beta$ -MnO<sub>2</sub> shows distinctly (although broadened) just before the main step to  $\alpha$ -Mn<sub>2</sub>O<sub>3</sub> occurs. The appearance of  $\beta$ -MnO<sub>2</sub> in this range is gradual and can also be seen in the shift of lines of  $\gamma$ -MnO<sub>2</sub> (Fig. 3).

Na-7 Å phyllo-manganate Na<sub>4</sub>Mn<sub>14</sub>O<sub>27</sub> · 9H<sub>2</sub>O shows a progressive weakening of the X-ray diffraction lines right from the beginning. The weakening is already distinct at 105°C and at 600°C the pattern was nearly vanished with the 7 Å (very broad) reflection remaining. At 870°C sharp reflections

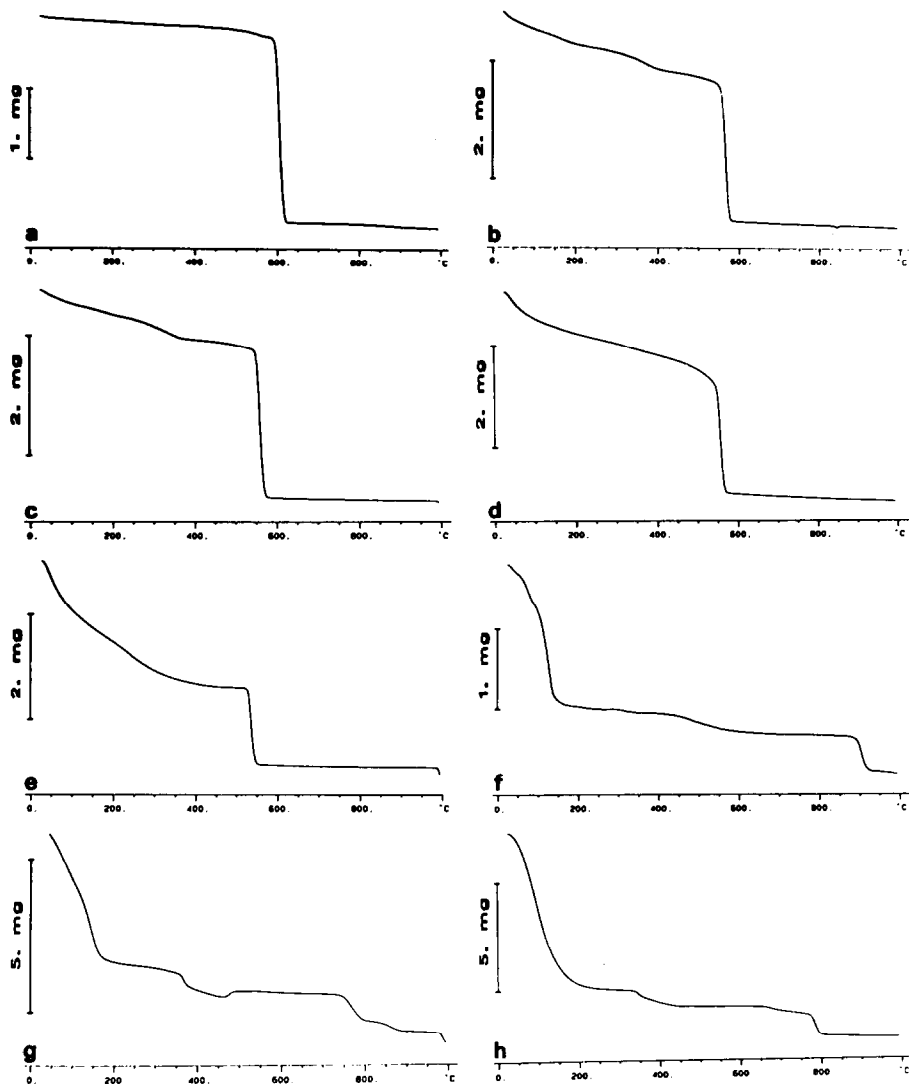


Fig. 2. Typical TG curves for (a)  $\beta$ - $\text{MnO}_2$  (refluxed) ( $\beta$ - $\text{MnO}_2$  Baker gives a virtually identical trace), (b)  $\gamma$ - $\text{MnO}_2$  (Faradiser WS), (c)  $\gamma$ - $\text{MnO}_2$  (refluxed), (d)  $\epsilon$ - $\text{MnO}_2$  (Faradiser M), (e)  $\epsilon$ - $\text{MnO}_2$  (ozone method), (f) Na 7 Å phyllosmanganate  $\text{Na}_4\text{Mn}_{14}\text{O}_{27}\cdot 9\text{H}_2\text{O}$ , (g) Glemser's " $\delta$ - $\text{MnO}_2$ " (finely divided 7 Å phyllosmanganate), (h) Z disordered phyllosmanganate after Murray.

of  $\text{Na}_2\text{Mn}_5\text{O}_{10}$  are fully developed and at 1000°C yet another pattern appears (Fig. 4).

The formation of  $\text{Na}_2\text{Mn}_5\text{O}_{10}$  is slow and can best be observed in isothermal runs (24 h, in standing air). The layer lattice of the starting product collapses at 150°C and only at 500°C does the new phase begin to appear. Its formation is complete at 600°C after 24 h (Fig. 5).

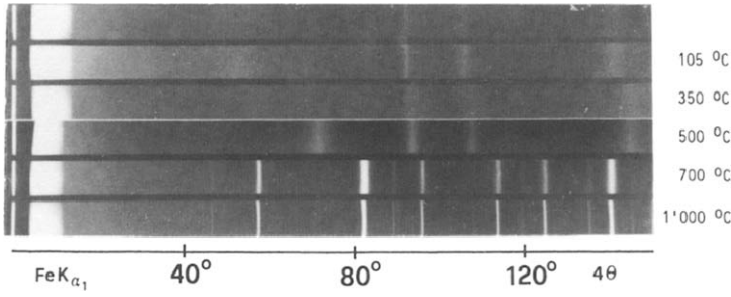


Fig. 3. X-Ray diffraction patterns of  $\epsilon$ -MnO<sub>2</sub> (ozone method) and its TG products (dynamic conditions).

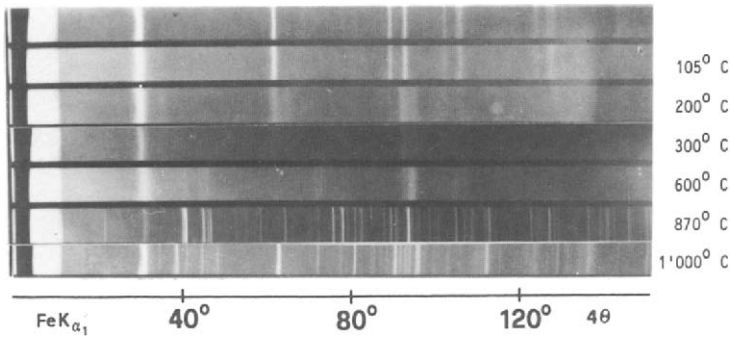


Fig. 4. X-Ray diffraction patterns of Na 7 Å phyllosilicate Na<sub>4</sub>Mn<sub>14</sub>O<sub>27</sub> · 9H<sub>2</sub>O and its TG products (dynamic conditions).

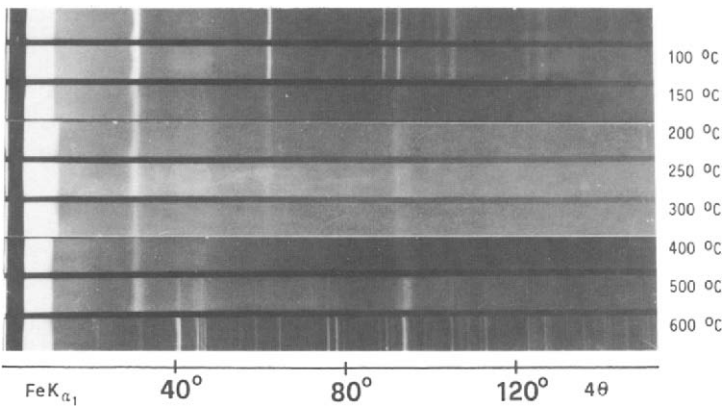


Fig. 5. Same as Fig. 4, but under isothermal conditions (24 h).



### 3.3. Electron microscopy

Although dramatic events may occur in TG curves, the electron microscopic morphology hardly changes up to 600°C or even further. We show this in the two most distinctive cases,  $\gamma$ -MnO<sub>2</sub> and 7 Å phyllomanganate. The prisms of  $\gamma$ -MnO<sub>2</sub> remain unaltered up to 500°C and only at 870°C do the particles show rounded contours indicating a sintering process (Fig. 6).

The platelets of 7 Å phyllomanganate remain unaltered up to 600°C. At 870°C a dramatic change has taken place. The platelets have recrystallized to prisms and long needles of Na<sub>2</sub>Mn<sub>5</sub>O<sub>10</sub> (Fig. 7).

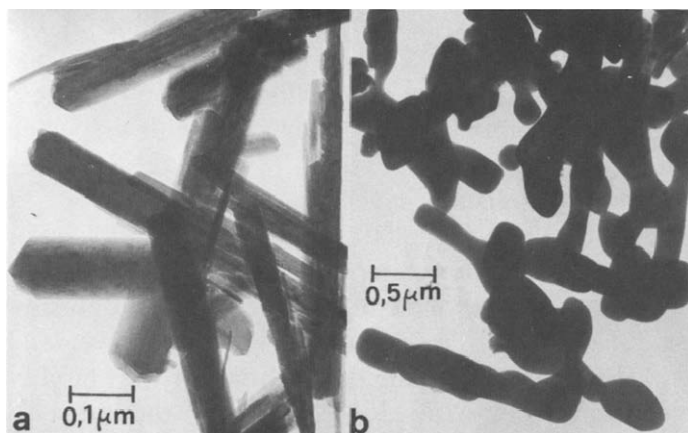


Fig. 6. Electron micrographs of (a)  $\gamma$ -MnO<sub>2</sub> (refluxed) and (b) its TG product at 870°C.

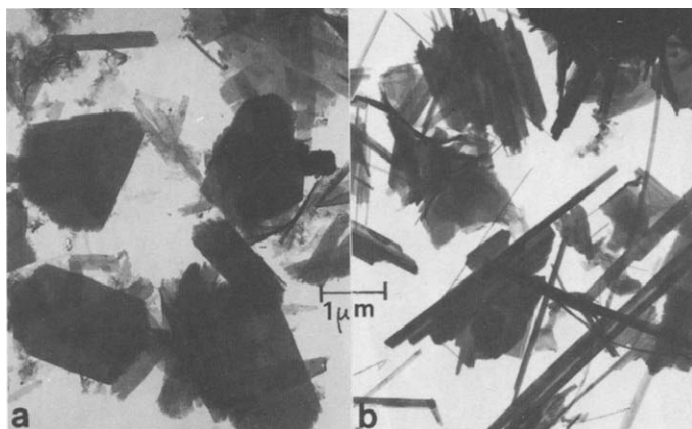


Fig. 7. Transmission electron micrographs of (a) Na 7 Å phyllomanganate Na<sub>4</sub>Mn<sub>14</sub>O<sub>27</sub> · 9H<sub>2</sub>O and (b) its TG product at 870°C.

## 4. DISCUSSION

### 4.1. Water loss

The comparison of the various curve types and the structures of the starting and final products lead us to the conclusion that three kinds of water can be observed in manganese dioxides. These types of water are released at different temperatures. (i) Adsorbed (loosely bound) molecular water desorbs from 25 to 105°C; (ii) interlayer water, still molecular, but more tightly bound, is released at temperatures overlapping with those of adsorption water release but extending up to 150–250°C; (iii) condensing of OH groups leads to the release of much more tightly bound water (which we call here OH-water) from 105 to 500°C and above (but this is obscured by the main step that takes place in this region).

Adsorbed water can be removed by careful drying (without affecting the  $\text{MnO}_2$ ) to one or several monomolecular layers and is then a function of the specific surface area of the  $\text{MnO}_2$ . The coarse  $\beta$ - $\text{MnO}_2$  (Baker) has less than 0.1% adsorbed water. The reflux  $\beta$ - $\text{MnO}_2$ , however, with a specific surface area of about  $6 \text{ m}^2 \text{ g}^{-1}$ , has a content of 0.78% adsorbed water which is about five times a monomolecular layer.

Interlayer water can only occur in layer lattices and is also molecular water. It begins to leave the lattice at low temperatures (just above 25°C) i.e. its loss overlaps in TG runs with that of adsorbed water, but its diffusion out of the lattice (even out of the collapsed lattice) is much slower and protracted to 150–250°C. This interlayer water is essential for the stability of the lattice and its release immediately leads to collapse of the lattice.

$\text{OH}^-$  groups in  $\gamma$ - and  $\epsilon$ - $\text{MnO}_2$  play an important role [12]. They replace  $\text{O}^{2-}$  ions in order to balance the  $\text{Mn}^{3+}$  ions substituting  $\text{Mn}^{4+}$  ions in these two mineral species. Prolonged heating (isothermal) in air or in  $\text{O}_2$  leads to oxidation of  $\text{Mn}^{3+}$  ions to  $\text{Mn}^{4+}$  and an equivalent amount of  $\text{OH}^-$  ions leaves as  $\text{H}_2\text{O}$  which we call OH-water. As mentioned, we have shown [11] that this process leads to the nucleation of technically undesirable  $\beta$ - $\text{MnO}_2$  which we also observe in dynamic experiments. The OH-water is thus an indicator of the electrochemical activity of a  $\text{MnO}_2$  sample, together with the particular phenomena in X-ray diffraction patterns that indicate a specific disorder. Both are essential for the applicability of a  $\text{MnO}_2$  for dry batteries. The disorder and the  $\text{Mn}^{4+}$  vacancies have been discussed at length by Rüetschi and Giovanoli [12] and more recently by Brenet [13].

### 4.2. Oxide transformations

The important mass loss in  $\beta$ -,  $\gamma$ - and  $\epsilon$ - $\text{MnO}_2$  in the main step is due to the transformation to  $\alpha$ - $\text{Mn}_2\text{O}_3$ . This new phase has a much larger crystallite size than the starting products  $\gamma$ - and  $\epsilon$ - $\text{MnO}_2$  which shows in

the sharp and intense X-ray lines in Fig. 3 at 700°C and beyond. Some sintering goes on until 1000°C, as indicated by the disappearance of the slight line-broadening observed in the 700°C product.

The question remains as to why some of our starting products begin to form  $\text{Mn}_3\text{O}_4$  near 1000°C even in  $\text{O}_2$  atmosphere. The investigation of all samples with energy dispersive X-ray spectroscopy has shown that industrial products may have  $\text{SiO}_2$  or  $\text{SiO}_4^{4-}$  contents of 0.1% or more. These species block solid state transformations as well as transformations in suspension as pointed out in ref. 11. The sulphate ion often encountered in industrial products also acts as an inhibitor.

The transformations in phyllomanganates are complicated. The  $\text{Na}_2\text{Mn}_5\text{O}_{10}$  phase needs for its formation (like  $\alpha\text{-Mn}_2\text{O}_3$ ) a total rearrangement of the lattice components. As there are  $\text{Na}^+$  ions to accommodate, this rearrangement is slow.

In Glemser's 7 Å phyllomanganate (" $\delta\text{-MnO}_2$ ") there are enough  $\text{K}^+$  ions to nucleate cryptomelane  $\text{KMn}_8\text{O}_{16}$ .

## 5. CONCLUSIONS

Thermogravimetry has been found to be a most valuable tool in characterizing (together with X-ray diffraction and electron microscopy) the manganese dioxides. The TG method helps considerably in understanding the processes involved in heating ("roasting") these compounds and is therefore important in evaluating electrochemically active manganese dioxides.

## ACKNOWLEDGEMENTS

We are grateful to the Wander-Hochschulstiftung Berne and the Portland Cement-Fabrik Laufen Foundation for financial support and to Mrs. Wild and Miss Ettinger for technical help.

## REFERENCES

- 1 O. Glemser, G. Gattow and H. Meisiek, *Z. Anorg. Allg. Chem.*, 309 (1961) 1.
- 2 G. Gattow and O. Glemser, *Z. Anorg. Allg. Chem.*, 309 (1961) 20.
- 3 G. Gattow and O. Glemser, *Z. Anorg. Allg. Chem.*, 309 (1961) 121.
- 4 R. Giovanoli, R. Maurer and W. Feitknecht, *Helv. Chim. Acta*, 50 (1967) 1072.
- 5 R. Giovanoli, K. Bernhard and W. Feitknecht, *Helv. Chim. Acta*, 51 (1968) 355.
- 6 R. Giovanoli, E. Stähli and W. Feitknecht, *Chimia*, 23 (1969) 264.
- 7 R. Giovanoli and U. Leuenberger, *Helv. Chim. Acta*, 52 (1969) 2333.
- 8 R. Giovanoli and E. Stähli, *Chimia*, 24 (1970) 49.
- 9 R. Giovanoli, E. Stähli and W. Feitknecht, *Helv. Chim. Acta*, 53 (1970) 209, 453.
- 10 J.W. Murray, *J. Colloid Interface Sci.*, 46 (1974) 357.
- 11 R. Giovanoli, in B. Schumm, H.J. Joseph and A. Kozawa (Eds.), *Proc. Manganese Dioxide Symp.*, Vol. 2, Tokyo, 1980, Cleveland Ohio, 1981, pp. 113–133.
- 12 P. Ruetschi and R. Giovanoli, *J. Electrochem. Soc.*, 135 (1988) 2663.
- 13 J. Brenet, *J. Power Sources*, 39 (1992) 349.